
Simulating GPS Radio Occultation Using 3-D Ray Tracing

R. Norman, J. Le Marshall, K. Zhang, C.S. Wang, B.A. Carter, Y. Li, and S. Gordon

Abstract

Numerical 3-D ray tracing techniques are commonly used for calculating the path of an electromagnetic signal in a medium specified by a refractive index that depends upon position. Numerical ray tracing is an important tool for applications of L-band frequency propagation such as GPS Radio Occultation (RO), where accurate and near real-time results are required. In this study, 3-D numerical ray tracing techniques are used to simulate GPS signals received by the Low Earth Orbit (LEO) satellites and to investigate their variability as a function of time and position due to the refractivity gradients in the ionosphere and the lower atmosphere. The GPS signal paths from the GPS to LEO satellites are simulated with an emphasis on the signal paths propagating through regions of the ionosphere where the refractive gradients are greatest. The effects of the Earth's magnetic field on the L-band RO propagation paths are also investigated.

Keywords

Ionosphere • Refractivity • Ray tracing • Radio occultation

1 Introduction

GPS Radio Occultation (RO) is an emerging space-based Earth observation technique with the potential for atmospheric profiling and meteorological applications. GPS RO uses GPS receivers onboard Low Earth Orbit (LEO) satellites to measure the radio signals transmitted from GPS satellites. The GPS consists of about 30 satellites traveling at an altitude of $\sim 20,200$ km orbiting the Earth twice a day

and continually transmit signals at the L-band frequencies 1.57542 GHz (L1), 1.2276 GHz (L2) and 1.17645 MHz (L5). Refractive gradients in the ionosphere and atmosphere affect the paths of the L-band electromagnetic signals transmitted from GPS satellites, causing the signals to bend in accordance to Snell's law. The bending of the ray paths in the ionosphere is due to electron density gradients. Refractivity in the lower atmosphere depends mainly upon the atmospheric pressure, temperature and the partial pressure of the water vapour.

The RO technique was initially developed for sounding planetary atmospheres and has aided NASA's planetary exploration programs to Venus, Mars and the outer planets (Fjeldbo et al. 1971; Phinney and Anderson 1968; Bird et al. 1992). The technique has been applied to determine the structure of the Earth's lower atmosphere and ionosphere (Hajj et al. 1994; Healy and Eyre 2000; Hardy et al. 1993; Hernandez-Pajares et al. 2000; Rocken et al. 1997) and to advance meteorological research (Cucurull et al. 2007; Le Marshall et al. 2010, 2012; Zhang et al. 2011).

R. Norman (✉) • K. Zhang • C.S. Wang • B.A. Carter • Y. Li • S. Gordon

Satellite Positioning for Atmosphere, Climate and Environment (SPACE) Research Centre, RMIT University, Melbourne, VIC, Australia

e-mail: robert.norman7@gmail.com

J. Le Marshall

Satellite Positioning for Atmosphere, Climate and Environment (SPACE) Research Centre, RMIT University, Melbourne, VIC, Australia

Bureau of Meteorology, Melbourne, VIC, Australia

Ionospheric RO retrievals and corrections remain a major challenge for the overall GPS RO technique. Atmosphere and ionosphere retrieval methods assume local spherical symmetry of the refractivity. The RO retrieval techniques fail to take into consideration the significant spatial and temporal variations in the ionospheric horizontal and vertical electron density gradients and the refractivity gradients in the lower atmosphere. At present, retrieval techniques do not take into account the birefringence effects on the signals in the ionosphere caused by the Earth's magnetic field.

The ionosphere is the region of the Earth's upper atmosphere located at altitudes between 60 and 1,500 km and is normally considered as the transition zone between our atmosphere and outer space, its primary source of ionization is incident ultra violet solar radiation. The ionosphere is highly dynamic and the study of "space weather" or "space climate" refers to the ionosphere's important connection to the Earth's atmosphere and its dynamic nature. The ionosphere thickens, changes its density, and supports a wide range of traveling disturbances, generated by the flux of incident ionizing solar radiation. The dynamic nature of the ionosphere is apparent on timescales of minutes and hours, as well as diurnally and seasonally. Some of the major features of the ionosphere are

the ionospheric electron density layers, equatorial anomaly, troughs of ionization and a range of traveling ionospheric disturbances.

This study focuses on GPS signal propagation and in particular the ionospheric and atmospheric effects on GPS signals. A new 3-D numerical ray tracing technique (Norman et al. 2013), based on Haselgroves equations, utilizing geometrical optics principles in anisotropic media is used to trace the GPS ray paths. Ray tracing techniques are commonly used for calculating the path of an electromagnetic signal in a medium specified by a position-dependent refractive index. In this study numerical 3-D ray tracing is used to trace L-band frequency paths with a sophisticated ionospheric model, namely the International Reference Ionosphere (IRI-2007) (Bilitza and Reinisch 2008). The effects due to ionospheric gradients and the Earth's magnetic field on GPS signal paths that are initialized with a negative elevation angle will be investigated. A simple exponential function with a scale height of 7.5 km and ground refractivity of 300 N-units is used to represent the lower atmosphere.

The phase refractive index in the ionosphere (n) is given by the Appleton-Lassen equation:

$$n^2 = 1 - \frac{X}{1 - iZ - \frac{Y_T^2}{2(1-X-iZ)} \pm \frac{1}{1-X-iZ} \sqrt{\left(\frac{Y_T^4}{4} + Y_L^2(1-X-iZ)^2\right)}} \quad (1)$$

where

X is proportional to the electron density,

Y is proportional to the Earth's magnetic field (longitudinal Y_L and transverse Y_T components)

Z is proportional to the collision frequency (ignored)

"+" generally represents the ordinary (O) mode and "-" generally represents the extraordinary (X) mode.

Refractivity $N = (n - 1) \times 10^6$ (N-units)

2 Results

The 3-D numerical ray tracing program incorporates the IRI-2007 model for the electron density in the ionosphere and a special version of the POGO 68/10 magnetic field Legendre model (found in the IRI-2007). Ray tracing was performed between a GPS and LEO satellite. The GPS satellite used had fixed geomagnetic coordinates (-66.4°N , 164°E) and was positioned to observe geomagnetic northward propagation. The LEO satellite utilized had an orbital altitude of 800 km. Ray tracing was performed for day 207 in year 2010 as inputs to the IRI-2007. Figure 1 shows the electron density with respect to height and geomagnetic latitude, for the fixed

geomagnetic longitude 164°E and ~ 1200 LT (local time). Notice the latitudinal, altitudinal and diurnal variations in the refractivity. The chosen ray tracing model constraints highlight the equatorial anomaly and the gradients in electron density. At night, ionosphere electron densities are weak; therefore the magnitude of the refractivity is reduced. This is evident in Fig. 2, which shows a vertical profile of the refractivity at 1200 LT and geomagnetic coordinates 35°N , 164°E . These coordinates represent the tangent point where the perigee height is ~ 100 km. The data points are in steps of 3 km starting from a height of 3 km up to a height of 870 km. The refractivity in the lower atmosphere is significant at heights < 30 km. The ionosphere is a dispersive medium and Fig. 2 shows the profiles of refractivity for the L1 and L2 band GPS frequencies. Figure 2 shows the GPS L1 band frequency, refractivity profiles of the ionosphere and how it can change both spatially and temporally. The green profile in Fig. 2 corresponds to the refractivity at geomagnetic coordinates 164°E , 0°N at 1200 LT.

From Fig. 2 the refractivity in the ionosphere is negative, refer to (1). At heights from 40 to 80 km refractivity is close to zero. The refractivity at the Earth's surface is approximately 300 N-units and decreases exponentially in the

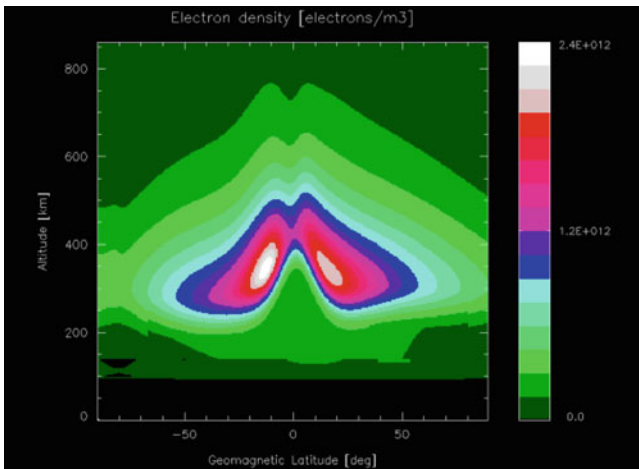


Fig. 1 Electron density from IRI-2007 for a geomagnetic longitude 164°E, 1200 LT, day 207 and year 2010

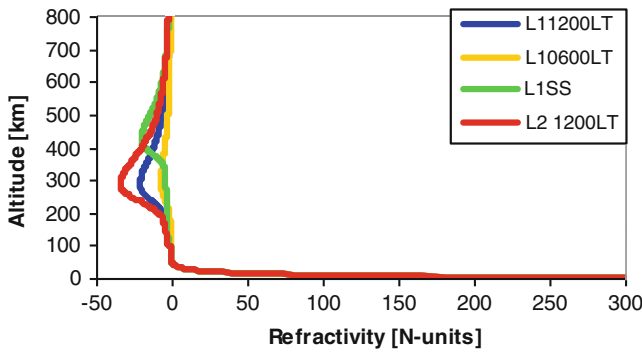


Fig. 2 Refractivity for a geomagnetic coordinates 164°E, 35°N at 0600 and 1200 LT and 164°E, 0°N at 1200LT for L1SS

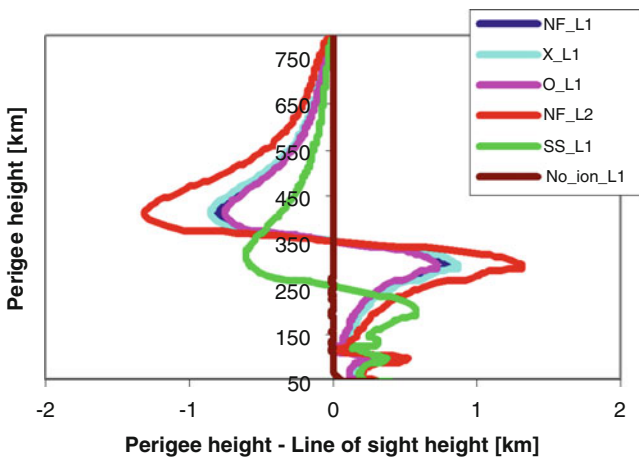


Fig. 3 RO ray tracing results showing perigee height versus perigee height—line of sight height

troposphere and stratosphere with a scale height of 7.5 km. The refractivity follows (1) above an altitude of 60 km.

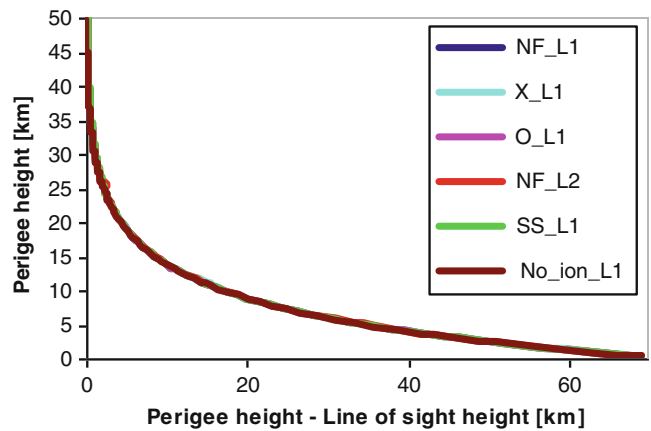


Fig. 4 RO ray tracing results showing perigee height versus perigee height—line of sight height, below a perigee height of 50 km

The impact parameter and tangent point are important parameters in RO retrieval algorithms. The impact parameter is the height of the closest approach of a ray path to the Earth’s surface and the tangent point is the ground position of the impact parameter. In ray tracing this point of closest approach of a ray path to the Earth’s surface is called the perigee height. In classical RO as the ray path traverses the ionosphere and atmosphere the impact parameter is shown to be above the line of sight between the GPS and LEO satellites. Ray tracing has proven this assumption incorrect (Norman et al. 2012), as the results in Fig. 3 clearly show that RO ray paths can be below the line of sight i.e., perigee height—line of sight < 0. Ray paths not traversing below hmF2 (height maximum of the F2 layer) will bend upwards as the lower parts of the signal path will be in a region of slightly higher electron density, thus lower refractivity, and will travel faster causing the signal to refract upwards away from the Earth. Figure 3 shows perigee heights versus the difference in perigee height when no refractive gradients are present. Ray tracing results are shown for the GPS L1 and L2 band frequencies as well as the L1 no field (NF), ordinary (O), extraordinary (X) and spherically stratified (SS) ionosphere paths. Notice that the O and X perigee heights are either side of the NF perigee heights. Figure 4 shows the results below 50 km, where the difference in perigee height and the line of sight height can be as much as 70 km due to the increased refractivity in the troposphere and boundary layer.

From Fig. 3 the differences in perigee height from the line of sight height in the ionosphere is less than 2 km. Figure 5 shows a zoomed in section of Fig. 4. From Fig. 5 the difference in perigee height can be tens of meters away from the true value if the ionosphere ignored.

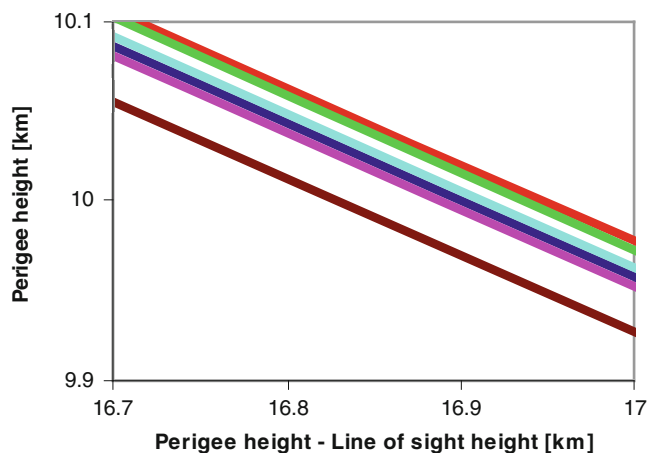


Fig. 5 A zoomed in section from Fig. 4

3 Conclusion

The effects of ionospheric gradients and birefringence on GPS L-band frequency RO propagation paths were investigated. In this study geomagnetic northward propagating signals were studied using a 3-D ray tracing technique incorporating the IRI-2007 and the POGO 68/10 magnetic field model to simulate RO ray paths. It was found that refractive gradients in the ionosphere can cause the perigee heights in the ionosphere to be below the GPS to LEO line of sight height. For RO ray paths with a perigee height of 10 km the ionosphere contributes ~ 50 m change to the perigee height and the magnetic field contributes ~ 15 m. Ray tracing combined with the best available ionospheric and magnetic field models is important for understanding the contributions of ionospheric gradients, atmospheric gradients and the Earth's magnetic field on GPS RO propagation paths.

Acknowledgements This work is supported in part by the Australian Space Research Program project of "Platform Technologies for Space, Atmosphere and Climate" endorsed to a research consortium led by RMIT University.

References

Bird MK, Asmar SW, Brenle JP, Edenhofer P, Funke O, Patzoid M, Volland H (1992) Ulysses radio occultation observations of the Io plasma torus during the Jupiter encounter. *Science* 257:1531–1535

- Bilitza D, Reinisch B (2008) International reference ionosphere 2007: improvements and new parameters. *Adv Space Res* 42(4):599–609
- Cucurull L, Derber JC, Treadon R, Purser RJ (2007) Assimilation of global positioning system radio occultation observations into NCEP's global data assimilation system. *Mon Weather Rev* 135:3174–93
- Fjeldbo G, Kliore AJ, Eshleman VR (1971) The neutral atmosphere of Venus as studied with Mariner V radio occultation experiments. *Astron J* 76:123–140
- Hajj GA, Ibanez-Meier R, Kursinski ER, Romans LJ (1994) Imaging the ionosphere with global positioning system. *Int J Imaging Syst Technol* 5:174–184
- Hardy KR, Hajj GA, Kursinski ER (1993) Accuracies of atmospheric profiles obtained from GPS occultations. In: *Proceedings of the ION-GPS 93 conference*, Institute of Navigation, Salt Lake City, pp 1545–1557
- Healy SB, Eyre JR (2000) Retrieving temperature, water vapor and surface pressure information from refractive index profiles derived by radio occultation: a simulation study. *Q J R Meteorol Soc* 126:1661–83
- Hernandez-Pajares M, Juan JM, Sanz J (2000) Improving the Abel inversion by adding ground GPS data to LEO radio occultations in ionospheric sounding. *Geophys Res Lett* 27:2473–2476
- Le Marshall J, Xiao Y, Norman R, Zhang K, Rea A, Cucurull L, Seecamp R, Steinle P, Puri K, Le T (2010) The beneficial impact of radio occultation observations on Australian region forecasts. *Aust Meteorol Oceanogr J* 60:121–125
- Le Marshall J, Xiao Y, Norman R, Zhang K, Rea A, Cucurull L, Seecamp R, Steinle P, Puri K, Le T (2012) The application of radio occultation for climate monitoring and numerical weather prediction in Australian region. *Aust Meteorol Oceanogr J* 62:323–334
- Norman RJ, Bennett JA, Dyson PL, Le Marshall J, Zhang K (2013) A ray-tracing technique for determining ray tubes in anisotropic media. *IEEE Trans Antennas Propag* 61(5):2664–2675
- Norman RJ, Dyson PL, Yizengaw E, Le Marshall J, Wang C-S, Carter B, Wen D, Zhang K (2012) Radio occultation measurements from the Australian micro satellite FedSat. *IEEE Trans Geosci Remote Sensing* 50(11):4832–4839. doi:10.1109/TGRS.2012.2194295
- Phinney RA, Anderson DL (1968) On the radio occultation method for studying planetary atmospheres. *J Geophys Res* 73:1819–1827
- Rocken C, Anthes R, Exner M, Hunt D, Sokolovskiy S, Ware R, Gorbunov M, Schreiner W, Feng D, Herman B, Kuo Y, Zou X (1997) Analysis and validation of GPS/MET data in the neutral atmosphere. *J Geophys Res* 102:29849–29866
- Zhang K, Fu E, Silcock D, Wang Y, Kuleshov Y (2011) An investigation of atmospheric temperature profiles in the Australian region using collocated GPS radio occultation and radiosonde data. *Atmos Meas Tech* 4:2087–2092